Impact of Statin Therapy on Plaque Characteristics as Assessed by Serial OCT, Grayscale and Integrated Backscatter–IVUS

Kousuke Hattori, MD,* Yukio Ozaki, MD,* Tevfik F. Ismail, MBBS,†
Masanori Okumura, MD,* Hiroyuki Naruse, MD,* Shino Kan, MD,* Makoto Ishikawa, MD,*
Tomoko Kawai, MD,* Masaya Ohta, MD,* Hideki Kawai, MD,* Tousei Hashimoto, MD,*
Yasushi Takagi, MD,* Junichi Ishii, MD,* Patrick W. Serruys, MD,‡ Jagat Narula, MD§

Toyoake, Japan; London, United Kingdom; Rotterdam, the Netherlands; and New York, New York

OBJECTIVES The purpose of this study was to evaluate the effect of statin treatment on coronary plaque composition and morphology by optical coherence tomography (OCT), grayscale and integrated backscatter (IB) intravascular ultrasound (IVUS) imaging.

BACKGROUND Although previous studies have demonstrated that statins substantially improve cardiac mortality, their precise effect on the lipid content and fibrous cap thickness of atherosclerotic coronary lesions is less clear. While IVUS lacks the spatial resolution to accurately assess fibrous cap thickness, OCT lacks the penetration of IVUS. We used a combination of OCT, grayscale and IB-IVUS to comprehensively assess the impact of pitavastatin on plaque characteristics.

METHODS Prospective serial OCT, grayscale and IB-IVUS of nontarget lesions was performed in 42 stable angina patients undergoing elective coronary intervention. Of these, 26 received 4 mg pitavastatin after the baseline study; 16 subjects who refused statin treatment were followed with dietary modification alone. Follow-up imaging was performed after a median interval of 9 months.

RESULTS Grayscale IVUS revealed that in the statin-treated patients, percent plaque volume index was significantly reduced over time (48.5 ± 10.4%, 42.0 ± 11.1%; p = 0.033), whereas no change was observed in the diet-only patients (48.7 ± 10.4%, 50.4 ± 11.8%; p = NS). IB-IVUS identified significant reductions in the percentage lipid volume index over time (34.9 ± 12.2%, 28.2 ± 7.5%; p = 0.020); no change was observed in the diet-treated group (31.0 ± 10.7%, 33.8 ± 12.4%; p = NS). While OCT demonstrated a significant increase in fibrous cap thickness (140 ± 42 μm, 189 ± 46 μm; p = 0.001), such changes were not observed in the diet-only group (140 ± 35 μm, 142 ± 36 μm; p = NS). Differences in the changes in the percentage lipid volume index (−6.8 ± 8.0% vs. 2.8 ± 9.9%, p = 0.031) and fibrous cap thickness (52 ± 32 μm vs. 2 ± 22 μm, p < 0.001) over time between the pitavastatin and diet groups were highly significant.

CONCLUSIONS Statin treatment induces favorable plaque morphologic changes with an increase in fibrous cap thickness, and decreases in both percentage plaque and lipid volume indexes.   (J Am Coll Cardiol Img 2012;5:169–77) © 2012 by the American College of Cardiology Foundation

The clinical benefit of lipid-lowering therapy with 3-hydroxy-3-methylglutaryl coenzyme A reductase inhibitors has been conclusively demonstrated by numerous large-scale, multi-center, randomized primary and secondary prevention clinical trials (1–5). Numerous grayscale intravascular ultrasound (IVUS) imaging studies have revealed that statins blunt the progression of atherosclerosis or even decrease the percentage of atheroma volume (6–11). However, radiofrequency analysis with integrated backscatter–

See page 178

IVUS (IB-IVUS) has demonstrated a substantial decrease in the lipid burden and an increase in the fibrous content of a plaque in response to statins (12,13). Although the lipid fraction of a plaque and the plaque volume are determinants of plaque instability, the presence of a thin fibrous cap is the hallmark of a high-risk plaque (14–19). IVUS lacks the spatial resolution to accurately assess small changes in fibrous cap thickness. On the other hand, a single study using optical coherence tomography (OCT) demonstrated that statin therapy after the onset of acute myocardial infarction resulted in an increase in fibrous cap thickness (20). OCT, however, lacks the penetration of IVUS, and it is conceivable that a combination of IVUS and OCT would offer a comprehensive account of alterations in plaque morphology in response to statin treatment.

METHODS

Study design and patient selection. This nonrandomized, case-control study prospectively enrolled 42 patients with stable angina undergoing elective percutaneous coronary intervention (PCI) to evaluate the effects of statin therapy on nontarget lesions. Of these, 26 received pitavastatin 4 mg/day and 16 who declined any form of lipid-lowering pharmacotherapy received dietary intervention alone. The low-density lipoprotein cholesterol (LDL-C)–lowering efficacy of pitavastatin is comparable to that of atorvastatin (8). Serial imaging was performed in nontarget lesions, first during PCI and subsequently after a median duration of 9 months. Discrete nonobstructive lesions (<50% stenosis by quantitative coronary angiography),

identified by angiography, IVUS, and OCT, >5 mm proximal or distal to the stented lesions that were not in tandem or diffuse were studied. All patients underwent grayscale and IB-IVUS as well as OCT imaging. Patients already established on lipid-lowering therapy and those with contraindications to repeat coronary angiography and intracoronary imaging were excluded. The study was approved by our institutional ethics committee, and all patients gave written informed consent.

Angiographic and intracoronary imaging procedures. A 7-F guiding catheter was introduced via the femoral approach after administration of 100 IU/kg intravenous heparin. Selective coronary angiography was performed after the intracoronary injection of nitrates. All the lesions were treated with stent implantation after which imaging procedures were performed. The techniques and devices used for PCI were left to the operator's discretion.

After the passage of a 0.014-inch guidewire across the lesion, the proximal occlusion balloon catheter was positioned proximal to the lesion and a 0.014-inch guidewire was removed and exchanged for a 0.016-inch OCT image wire (LightLab Imaging, Westford, Massachusetts) (21,22). After the careful passage of a 0.016-inch OCT image wire through the lesion, a proximal occlusion balloon catheter was inflated, and then lactated Ringer's solution was continuously flushed through the lumen to remove blood flow. Motorized pull-back was started at a rate of 1.0 mm/s for a length of 30 mm. Non–PCI-related plaques (at least 5 mm proximal or distal to the PCI site) with readily identifiable nearby landmarks to facilitate serial imaging were studied. The images were saved in the OCT image system digitally for subsequent analysis (18,22–26). After OCT, a mechanical IVUS imaging catheter (40 MHz, 2.5-F, Boston Scientific, Natick, Massachusetts) was introduced over a 0.014-inch guidewire and positioned distal to the lesion (8,27,28). Lesion geometry was then imaged by using motorized pull-back (0.5 mm/s). For IB-IVUS image acquisition, a personal computer equipped with custom software (IB-IVUS, YD Co. Ltd., Nara, Japan) was connected to the IVUS imaging system (ClearView, Boston Scientific) to obtain radiofrequency signal output, signal trigger output, and video image output. IVUS images and data were stored electronically for offline analysis.

Image analysis. Intracoronary image analysis was performed by the consensus of 3 experienced
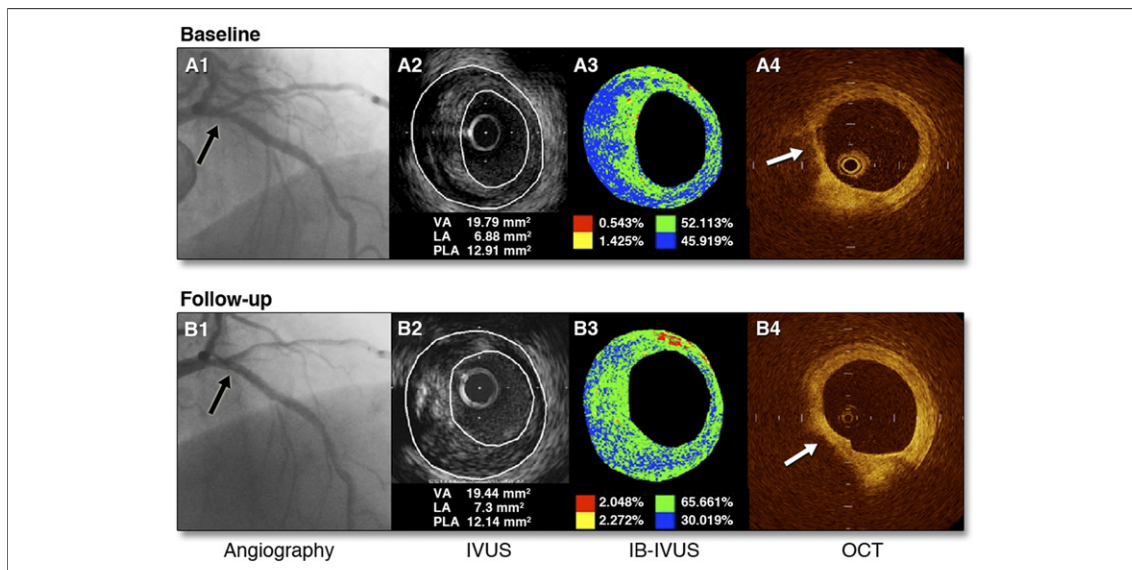
Figure 1. Coronary Angiographic, Grayscale IVUS, IB-IVUS, and OCT at Baseline and Follow-Up for the Pitavastatin Group

While no significant difference was found between baseline and follow-up angiography (**A1, B1**), plaque volume index (i.e., plaque area in this slice) decreased from 12.9 mm² to 12.1 mm² by grayscale IVUS during follow-up (**A2 and B2**). Lipid (**blue**) volume index decreased from 45.9% to 30.0%, while fibrous (**green**) volume index increased from 52.1% to 65.6% by IB-IVUS (**A3 and B3**). OCT revealed that the fibrous cap thickness increased from 80 μm to 220 μm during follow-up (**arrows in A4 and B4**). IB-IVUS = integrated backscatter–intravascular ultrasound; IVUS = intravascular ultrasound; LA = lumen area; OCT = optical coherence tomography; PLA = plaque area; VA = vessel area.

blinded observers (Y.O., M.O., K.H.) with no access to clinical records during assessment (Fig. 1). In OCT images, fibrous cap thickness was assessed (19,20,22). IVUS-verified cross-sectional lumen area was defined as the integrated area central to the intimal leading edge echo (27,28). The total vessel cross-sectional area was defined as the area inside the interface between the plaque-media complex and adventitia (27,28). The plaque area was defined as the vessel area minus the lumen area. Vascular
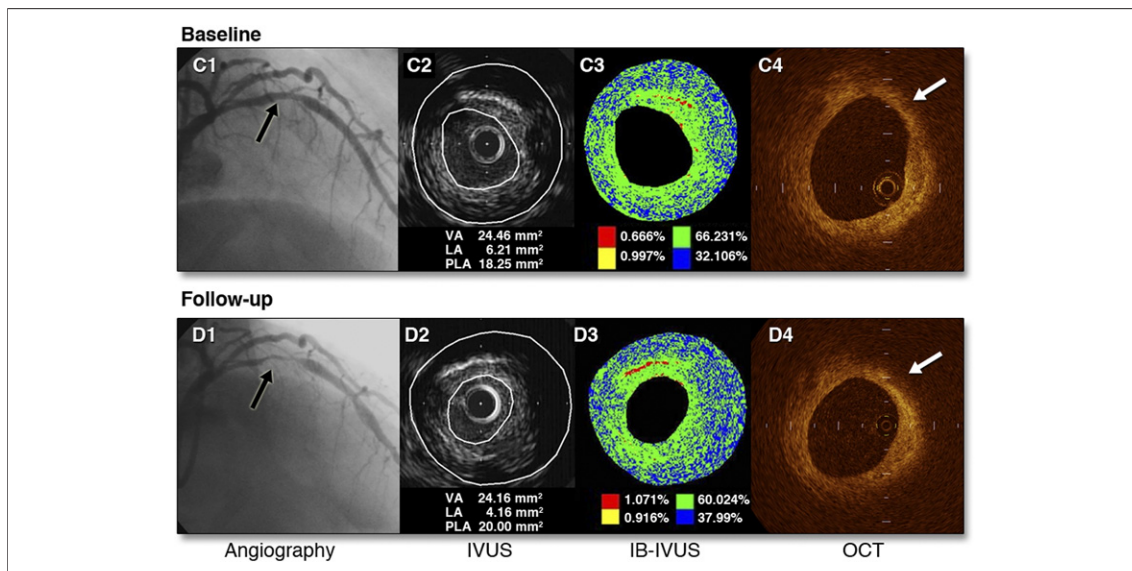
Figure 2. Coronary Angiographic, Grayscale IVUS, IB-IVUS, and OCT at Baseline and Follow-Up for the Dietary Group

Whilst significant progression was observed by angiography during follow-up (**C1 and C2**), plaque volume index (e.g., plaque area in this slice) increased from 18.2 to 20.0 mm² by grayscale IVUS during follow-up (**C2 and D2**). Lipid (**blue**) volume index increased from 32.1% to 37.9%, whereas fibrous (**green**) volume index decreased from 66.2% to 60.0% by IB-IVUS (**C3 and D3**). OCT revealed that the fibrous cap thickness of 110 μm did not change during follow-up (**arrows in C4 and D4**). Abbreviations as in Figure 1.

volume and lumen volumes were then calculated using Simpson's rule. The plaque volume was calculated by subtracting the lumen volume from the vascular volume. All values were indexed for lesion

Table 1. Baseline Demographic and Clinical Characteristics

	Pitavastatin	Diet therapy	p Value
No. of patients	26	16	—
No. of lesions	26	16	—
Age, yrs	66 ± 7.8	68 ± 6.2	0.194
Male	25 (96.1)	13 (81.3)	0.110
Follow-up period, months	9.0 (8.0–9.0)	9.0 (7.5–9.6)	0.641
Diabetes	9 (34.6)	4 (25.0)	0.513
HbA$_{1C}$ level, %	6.0 ± 1.0	5.7 ± 0.9	0.229
Hypertension, mm Hg	13 (50.0)	9 (56.3)	0.694
SBP	129 ± 17	140 ± 20	0.061
DBP	74 ± 10	78 ± 13	0.313
SBP at follow-up	121 ± 15	128 ± 13	0.104
DBP at follow-up	69 ± 13	76 ± 9	0.067
Smoking			
Nonsmoker	12 (46.2)	5 (31.2)	0.339
Ex-smoker	7 (26.9)	4 (25.0)	0.891
Current smoker	7 (26.9)	7 (43.8)	0.261
Quit at follow-up	3 (11.5)	4 (25.0)	0.256
Contined at follow-up	4 (15.4)	3 (18.8)	0.776
Lipid profile, mg/dl			
Total cholesterol	197 ± 46	200 ± 40	0.806
LDL-C	134 ± 40	122 ± 25	0.305
HDL-C	46 ± 11	59 ± 16	0.005
LDL-C/HDL-C ratio	3.08 ± 1.16	2.20 ± 0.65	0.009
Triglycerides	147 ± 48	117 ± 69	0.094
Stent type			
DES	24 (92.3)	13 (81.2)	0.282
BMS	2 (7.7)	3 (18.8)	0.282
Medications at follow-up/after index PCI			
Aspirin	26/26 (100)	16/16 (100)	1.000
Clopidogrel	9/9 (100)	6/7 (85.7)	0.241
Ticlopidine	13/14 (92.8)	7/9 (77.8)	0.294
Beta-blocker	12/12 (100)	11/11 (100)	1.000
ARB or ACEI	18/18 (100)	7/7 (100)	1.000
CCB	9/10 (90)	2/2 (100)	0.640
Major adverse cardiac events			
Death	0 (0)	0 (0)	1.000
MI	0 (0)	0 (0)	1.000
Restenosis rate	4 (15.4)	2 (12.5)	0.795
TLR	4 (15.4)	2 (12.5)	0.795
TVR	4 (15.4)	3 (18.8)	0.776
CABG	0 (0)	0 (0)	1.000

Values are mean ± SD, n (%), median (interquartile range), or n/N (%).
ACEI = angiotensin-converting enzyme inhibitor; ARB = angiotensin II receptor blocker; BMS = bare metal stent; CABG = coronary artery bypass grafting; CCB = calcium channel blocker; DBP = diastolic blood pressure; DES = drug-eluting stent; HDL-C = high-density lipoprotein cholesterol; LDL-C = low-density lipoprotein cholesterol; MI = myocardial infarction; PCI = percutaneous coronary intervention; SBP = systolic blood pressure; TLR = target lesion revascularization; TVR = target vessel revascularization.

length to give the vascular volume index, lumen volume index, and plaque volume index.

Integrated backscatter values for each tissue component were calculated as an average power using a fast Fourier transform of the frequency component of backscattered signal from a small volume of tissue (12,13). The percentage of fibrous volume (fibrous volume/plaque volume) and the percentage of lipid volume (lipid volume/plaque volume) were automatically calculated by the IB-IVUS system. The percentage of the high-signal volume (a part of the calcification on the inner surface that could be measured with the formula of IB-IVUS/plaque volume) was also automatically calculated by IB-IVUS as a high-signal volume (12,29,30). The percentage fibrous volume, the percentage lipid volume, and the high-signal volume were calculated using Simpson's rule. All values were indexed for lesion length to give the percentage fibrous volume index, the percentage lipid volume index, and the percentage high-signal volume index.

Statistical analysis. Data were analyzed using the SAS statistical software package version 9.1 (SAS Institute, Cary, North Carolina). All continuous values are expressed as mean ± SD for normally distributed variables and median ± interquartile range for nonparametric data. The Kolmogorov-Smirnov test was used to assess the normality of continuous data. Differences in categorical variables were assessed using the chi-square test and Fisher exact test as appropriate. Differences between paired continuous data were assessed using the paired Student *t* test. Between-group comparisons were made using the independent-samples *t* test or Mann-Whitney *U* test as appropriate. We used linear regression analysis to assess relationships between the percentage change in LDL-C during follow-up and several factors, including the percentage change in the coronary plaque volume index by grayscale IVUS, the percentage change in the lipid volume index by IB-IVUS, the percentage change in the fibrous volume index by IB-IVUS, and the percentage change in fibrous cap thickness by OCT. Analysis of covariance was used to adjust for differences in baseline lipid profiles between groups. Two-tailed p values <0.05 were considered significant.

RESULTS

Clinical characteristics. Serial intracoronary imaging follow-up was performed at a median duration of

9.0 months (interquartile range, 7.8 to 9.0 months) in all 42 patients. The baseline clinical and demographic characteristics of the treatment and control groups are summarized in Table 1. Both groups were comparable with respect to baseline characteristics, except for the presence of a higher high-density lipoprotein cholesterol level and subsequently lower LDL-C/high-density lipoprotein cholesterol ratio in the dietary treatment group. Of the 26 patients in the pitavastatin arm, 24 (92%) underwent PCI with drug-eluting stents and 2 (8%) received bare metal stents. Of the 16 patients with diet modification, 13 (81%) received drug-eluting stents and the remaining 3 (19%) received bare metal stents; there was no difference in the use of drug-eluting stent or bare metal stent implantation between the 2 groups (p = 0.282) (Table 1). A comparable number of patients in both groups experienced restenosis: 4 (15.4%) in the pitavastatin group and 2 (12.5%) in the diet-only group (p = 0.795). All 6 of these patients underwent repeat PCI of restenotic lesions; therefore, the target lesion revascularization rate was comparable in both groups. One patient in the diet-only group had a new significant lesion proximal to the original target lesion necessitating PCI. Therefore, target vessel revascularization including target lesion revascularization was needed in 4 patients (15.4%) in the pitavastatin group and 3 patients (18.7%) in the diet-only group (p = 0.776).

Lesion characteristics. Baseline lesion dimensions (assessed by grayscale IVUS) and plaque composition (assessed by IB-IVUS) were comparable for the 2 groups (Table 2). Fibrous cap thickness in both groups was also similar. In the treatment arm, pitavastatin resulted in significant reductions in total cholesterol, LDL-C as well as a significant increase in high-density lipoprotein cholesterol, but there was no appreciable change in triglyceride levels (Table 3). In comparison, in the dietary therapy control arm, there was no significant change in any component of the lipid profile between baseline and follow-up (Table 3).

Lipid-lowering therapy was associated with a significant decrease in the percentage plaque volume index by grayscale IVUS and the percentage plaque lipid area by IB-IVUS (Table 3). The percentage plaque volume index was reduced from 48.5 ± 10.4% to 42.0 ± 11.1% (p < 0.05) over time in the statin-treated arm; no change was observed in the diet-only patients (48.7 ± 10.4%, 50.4 ± 11.8%; p = NS). IB-IVUS revealed a significant

Table 2. Baseline Intracoronary Imaging Data			
Baseline	**Pitavastatin**	**Diet Therapy**	**p Value**
Target plaque location			
LAD	15 (57.7)	5 (31.3)	0.078
LCx	0 (0.0)	2 (12.5)	—
RCA	11 (42.3)	9 (56.3)	—
IVUS measurements, mm³/mm			
VVI	16.8 ± 4.1	17.6 ± 5.6	0.559
LVI	8.7 ± 2.8	9.2 ± 3.8	0.631
PVI	8.1 ± 2.4	8.5 ± 2.9	0.639
% PVI, %	48.5 ± 10.4	48.7 ± 10.4	0.963
Lesion length, mm	6.4 ± 2.6	6.1 ± 2.8	0.762
IB-IVUS analysis, %			
Lipid volume index	34.9 ± 12.2	31.0 ± 10.7	0.298
Fibrous volume index	63.9 ± 11.7	67.2 ± 9.5	0.348
OCT measurements			
Fibrous cap thickness, μm	140 ± 42	140 ± 35	0.997

Values are n (%) or mean ± SD.
IB-IVUS = integrated backscatter intravascular ultrasound; IVUS = intravascular ultrasound; LAD = left anterior descending coronary artery; LCx = left circumflex coronary artery; LVI = lumen volume index; OCT = optical coherence tomography; PVI = plaque volume index; %PVI = plaque volume index divided by vascular volume index; RCA = right coronary artery; VVI = vascular volume index.

decrease in the percentage lipid volume index from 34.9 ± 12.2% to 28.2 ± 7.5% (p < 0.05) over time; no change was apparent in the diet-only group (31.0 ± 10.7% and 33.8 ± 12.4%; p = NS). Although OCT demonstrated a significant increase in fibrous cap thickness (140 ± 42 μm and 189 ± 46 μm; p < 0.001), such changes were not observed in the diet-only group (140 ± 35 μm and 142 ± 36 μm; p = NS). Differences in the changes in the percentage lipid volume index from −6.8 ± 8.0% to 2.8 ± 9.9% (p = 0.03) and fibrous cap thickness from 52 ± 32 μm to 2 ± 22 μm (p < 0.001) between the pitavastatin and diet-only groups on serial follow-up were highly significant (Figs. 1 and 2).

We also examined the correlation between the percentage change in LDL-C and the change in several parameters. Figure 3 indicates that the percentage change in LDL-C had a significant positive correlation with the percentage change in the plaque volume index by grayscale IVUS (r = 0.39, p = 0.011) and with the percentage change in the lipid volume index by IB-IVUS (r = 0.40, p = 0.008). The percentage change in LDL-C also showed a significant negative correlation with the percentage change in the fibrous volume index by IB-IVUS (r = −0.38, p = 0.013) and the percentage change in fibrous cap thickness by OCT (r = −0.40, p = 0.010).

Table 3. Serial Changes in Lipid Profile, Grayscale IVUS, IB-IVUS, and OCT Findings

	Pitavastatin			Diet Therapy				Pitavastatin*	Diet Therapy*	p Value†
	Baseline	Follow-Up	p Value	Baseline	Follow-Up	p Value				
Lipid profile, mg/dl										
Total cholesterol	197 ± 46	164 ± 24	0.002	200 ± 40	195 ± 33	0.680	Change in total cholesterol	−32.7 ± 43	−5.4 ± 49	0.026
LDL-C	134 ± 40	89 ± 23	0.001	122 ± 25	121 ± 30	0.949	Change in LDL-C	−44.5 ± 30	−0.6 ± 34	<0.001
HDL-C	46 ± 11	58 ± 16	0.004	59 ± 16	53 ± 14	0.331	Change in HDL-C	11.6 ± 13	−5.1 ± 9	0.001
LDL-C/HDL-C ratio	3.08 ± 1.16	1.67 ± 0.61	0.001	2.20 ± 0.65	2.41 ± 0.82	0.422	Change in LDL-C/HDL-C	−1.41 ± 0.76	0.21 ± 0.71	<0.001
Triglycerides	147 ± 48	137 ± 82	0.569	117 ± 69	129 ± 71	0.610	Change in triglycerides	−10.7 ± 70	12.8 ± 107	0.422
IVUS measurements, mm³/mm										
VVI	16.8 ± 4.1	15.9 ± 4.1	0.483	17.6 ± 5.6	17.4 ± 6.0	0.905	Change in VVI	−0.8 ± 1.7	−0.3 ± 1.9	0.185
LVI	8.7 ± 2.8	9.3 ± 3.0	0.469	9.2 ± 3.8	9.4 ± 5.6	0.905	Change in LVI	0.6 ± 1.4	0.2 ± 3.2	0.746
PVI	8.1 ± 2.4	6.7 ± 2.5	0.050	8.5 ± 2.9	8.9 ± 3.8	0.740	Change in PVI	−1.4 ± 1.2	0.4 ± 1.5	<0.001
% PVI, %	48.5 ± 10.4	42.0 ± 11.1	0.033	48.7 ± 10.4	50.4 ± 11.8	0.670	Change in %PVI	−6.5 ± 6.2	1.7 ± 5.6	<0.001
IB-IVUS analysis, %										
Lipid volume index	34.9 ± 12.2	28.2 ± 7.5	0.020	31.0 ± 10.7	33.8 ± 12.4	0.506	Change in percentage lipid volume index	−6.8 ± 8.0	2.8 ± 9.9	0.031
Fibrous volume index	63.9 ± 11.7	70.0 ± 7.4	0.029	67.2 ± 9.5	64.1 ± 11.6	0.419	Change in percentage fibrous volume index	6.1 ± 7.3	−3.1 ± 9.2	0.014
OCT measurements										
Fibrous cap thickness, μm	140 ± 42	189 ± 46	0.001	140 ± 35	142 ± 36	0.861	Change in thickness	52 ± 32	2 ± 22	<0.001

Values are mean ± SD. *Value at follow-up minus value at baseline. †p Value adjusted for differences in baseline HDL-C.
Abbreviations as in Table 2.

DISCUSSION

Plaque regression and stabilization are expected to be the key mechanisms underlying the clinical benefit of lipid-lowering therapy with statins. Plaques susceptible to rupture are characterized by thin fibrous caps and a high lipid burden (31–33). Previous studies using grayscale IVUS demonstrated that significant reductions in plaque volume occur even after relatively short periods of therapy with different statins. On the other hand, radiofrequency IVUS analyses have confirmed that statins induce favorable changes in the plaque composition with a decrease in the lipid volume and an increase in the fibrous content (12,30). In the present study, we observed a significant correlation between LDL-C and a reduction in plaque and lipid volume. However, there was a significant negative correlation between the percentage decrease in LDL-C and the percentage increase in the fibrous volume and the percentage increase in fibrous cap thickness.

The magnitude of the decrease in the plaque volume index with pitavastatin in our study (−6.5 ± 6.2%) was similar to that in the JAPAN-ACS (Japanese Assessment of Pitavastatin and Atorvastatin in Acute Coronary Syndrome) study (−5.7 ± 6.3%) (8) and to the increase in the fibrous cap thickness seen in a recent OCT study (20) of acute myocardial infarction patients. Our study had the distinct advantage of using both IB-IVUS and OCT imaging modalities for better plaque characterization and the same statin at a consistent dose of 4 mg pitavastatin to minimize the possibility of varying responses to different statins of different potency and dose. We also managed to obtain complete imaging follow-up in all patients at 9 months after treatment.

The use of OCT to assess fibrous cap thickness is superior to IVUS because the spatial resolution of IVUS is only 100 μm, and vulnerable fibrous caps are typically <65 μm thick (34,35). IVUS is therefore unable to resolve small changes in fibrous cap thickness. Our data suggest that statins confer a beneficial increase in fibrous cap thickness. This provides valuable mechanistic insights into the potentially beneficial effects of statins, which could be used to benchmark future investigational agents that target plaque instability. This finding seems to support data from a previous study using CT angiography that demonstrated a substantial decrease in plaque volume in response to statin therapy (36). This preliminary study suggested that even low-dose statin use resulted in significant changes in plaque morphology. Statin treatment resulted in significant reduction of low attenuation
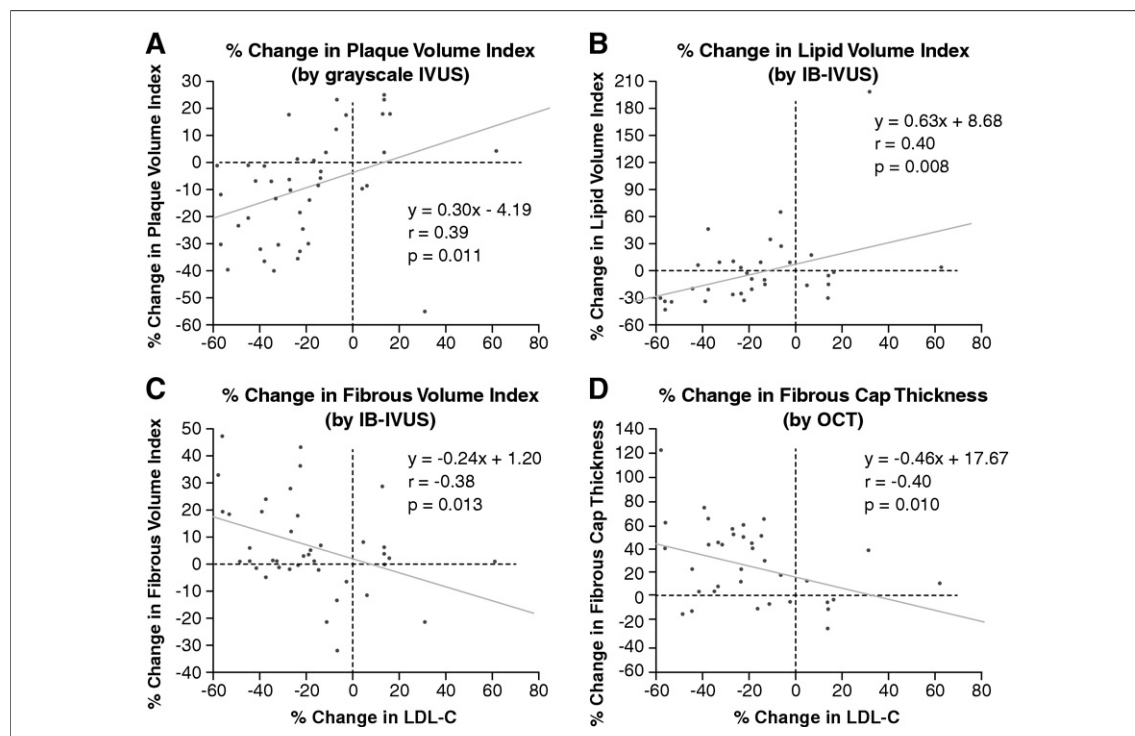
Figure 3. Relationship Between the Percentage of Change in LDL-C and Percentage of Grayscale IB-IVUS, and OCT Parameters

Relationship between percentage change in LDL-C and percentage change in plaque volume index by grayscale IVUS (**A**), percentage change in the lipid volume index by IB-IVUS (**B**), percent change in the fibrous volume index by IB-IVUS (**C**), and percentage change in fibrous cap thickness by OCT (**D**). Significant modest correlation was observed between the percentage change in LDL-C and all 4 parameters. LDL-C = low-density lipoprotein cholesterol; other abbreviations as in Figure 1.

plaque volume (IVUS equivalent of necrotic core component in computed tomography angiography) and in turn an absolute decrease in plaque volume. These changes in low attenuation and total plaque volume occurred when no significant change was observed in the lumen size, even if the changes in the lipid profile were not substantial. Somewhat similar results were reported from 18-fluorodeoxyglucose imaging of the carotid vasculature, which showed significant resolution of plaque inflammation in response to statin therapy; plaque inflammation remained unchanged after dietary intervention (37,38). Fibrous cap reinforcement and resolution of inflammation could be interrelated through cytokine and metalloproteinase attenuation, which is also known to be associated with statin therapy (39).

Study limitations. First, the number of patients studied is relatively small; however, this reflects the cost and logistical difficulties inherent in performing multimodality invasive intracoronary imaging. Second, given the established clinical benefit of lipid-lowering therapy, it would have been unethical to withhold treatment from the control group or to use a crossover design. We therefore relied on patients

who could not tolerate or had declined lipid-lowering therapy for our control group, raising the possibility of selection bias. Another possible study design could have used 2 different doses of same statins or 2 different statins for comparison of the efficacy of intervention on plaque instability. Nevertheless, the treatment and control groups in our study were very comparable with respect to important baseline clinical and lesion characteristics. Finally, over the short duration of this study, it was not possible to assess the significance of these changes with respect to event-driven, hard clinical endpoints. Nevertheless, such changes seen in the lipid profile have been previously established to translate into substantial decreases in clinical events with drugs in this class, and in this regard, pitavastatin has been shown to be noninferior to older statins.

CONCLUSIONS

Treatment with pitavastatin in patients with stable angina induces significant plaque regression and, by decreasing plaque lipid content and increasing plaque fibrous cap thickness, induces plaque stabilization. The use of serial multimodality intracoronary imaging

provides significant insights into the mechanisms underlying the clinical benefits of statins. Further work is required to prospectively correlate these changes with long-term clinical outcomes.

Acknowledgments

The authors are grateful to all the staff of the catheterization laboratory, Coronary Care Unit, and cardiac wards at the Fujita Health University Hospital for their dedication and contribution. The authors also wish to thank Professor Shuji Hashimoto and Professor Hitoshi Hishida for their helpful advice.

REFERENCES

1. Randomised trial of cholesterol lowering in 4444 patients with coronary heart disease: the Scandinavian Simvastatin Survival Study (4S). Lancet 1994;344:1383-9.
2. Sacks FM, Pfeffer MA, Moye LA, et al. The effect of pravastatin on coronary events after myocardial infarction in patients with average cholesterol levels. Cholesterol and Recurrent Events Trial investigators. N Engl J Med 1996;335:1001–9.
3. Streja L, Packard CJ, Shepherd J, Cobbe S, Ford I. Factors affecting low-density lipoprotein and high-density lipoprotein cholesterol response to pravastatin in the West Of Scotland Coronary Prevention Study (WOSCOPS). Am J Cardiol 2002;90:731–6.
4. Ridker PM, Danielson E, Fonseca FA, et al. Rosuvastatin to prevent vascular events in men and women with elevated C-reactive protein. N Engl J Med 2008;359:2195–207.
5. Tung P, Wiviott SD, Cannon CP, Murphy SA, McCabe CH, Gibson CM. Seasonal variation in lipids in patients following acute coronary syndrome on fixed doses of Pravastatin (40 mg) or Atorvastatin (80 mg) (from the Pravastatin or Atorvastatin Evaluation and Infection Therapy-Thrombolysis In Myocardial Infarction 22 [PROVE IT-TIMI 22] Study). Am J Cardiol 2009;103:1056–60.
6. Nissen SE, Tuzcu EM, Schoenhagen P, et al. Effect of intensive compared with moderate lipid-lowering therapy on progression of coronary atherosclerosis: a randomized controlled trial. JAMA 2004;291:1071–80.
7. Nissen SE, Nicholls SJ, Sipahi I, et al. Effect of very high-intensity statin therapy on regression of coronary atherosclerosis: the ASTEROID trial. JAMA 2006;295:1556–65.
8. Hiro T, Kimura T, Morimoto T, et al. Effect of intensive statin therapy on regression of coronary atherosclerosis in patients with acute coronary syndrome: a multicenter randomized trial evaluated by volumetric intravascular ultrasound using pitavastatin versus atorvastatin (JAPAN-ACS [Japan assessment of pitavastatin and atorvastatin in acute coronary syndrome] study). J Am Coll Cardiol 2009;54:293–302.
9. Rodriguez-Granillo GA, de Winter S, Bruining N, et al. Effect of perindopril on coronary remodelling: insights from a multicentre, randomized study. Eur Heart J 2007;28:2326–31.
10. Schoenhagen P, Tuzcu EM, Apperson-Hansen C, et al. Determinants of arterial wall remodeling during lipid-lowering therapy: serial intravascular ultrasound observations from the Reversal of Atherosclerosis with Aggressive Lipid Lowering Therapy (REVERSAL) trial. Circulation 2006;113:2826–34.
11. Garcia-Garcia HM, Costa MA, Serruys PW. Imaging of coronary atherosclerosis: intravascular ultrasound. Eur Heart J 2010;31:2456–69.
12. Kawasaki M, Sano K, Okubo M, et al. Volumetric quantitative analysis of tissue characteristics of coronary plaques after statin therapy using three-dimensional integrated backscatter intravascular ultrasound. J Am Coll Cardiol 2005;45:1946–53.
13. Amano T, Matsubara T, Uetani T, et al. Impact of metabolic syndrome on tissue characteristics of angiographically mild to moderate coronary lesions integrated backscatter intravascular ultrasound study. J Am Coll Cardiol 2007;49:1149–56.
14. Virmani R, Kolodgie FD, Burke AP, Farb A, Schwartz SM. Lessons from sudden coronary death: a comprehensive morphological classification scheme for atherosclerotic lesions. Arterioscler Thromb Vasc Biol 2000;20:1262–75.
15. Narula J, Willerson JT. Prologue: detection of vulnerable plaque. J Am Coll Cardiol 2006;47:C1.
16. Schaar JA, Muller JE, Falk E, et al. Terminology for high-risk and vulnerable coronary artery plaques. Report of a meeting on the vulnerable plaque, June 17 and 18, 2003, Santorini, Greece. Eur Heart J 2004;25:1077–82.
17. Kume T, Akasaka T, Kawamoto T, et al. Assessment of coronary arterial plaque by optical coherence tomography. Am J Cardiol 2006;97:1172–5.
18. Kubo T, Imanishi T, Takarada S, et al. Assessment of culprit lesion morphology in acute myocardial infarction: ability of optical coherence tomography compared with intravascular ultrasound and coronary angioscopy. J Am Coll Cardiol 2007;50:933–9.
19. Ozaki Y, Okumura M, Ismail TF, et al. Coronary CT angiographic characteristics of culprit lesions in acute coronary syndromes not related to plaque rupture as defined by optical coherence tomography and angioscopy. Eur Heart J 2011;32:2814–23.
20. Takarada S, Imanishi T, Kubo T, et al. Effect of statin therapy on coronary fibrous-cap thickness in patients with acute coronary syndrome: assessment by optical coherence tomography study. Atherosclerosis 2009;202:491–7.
21. Ozaki Y, Okumura M, Ismail TF, et al. The fate of incomplete stent apposition with drug-eluting stents: an optical coherence tomography-based natural history study. Eur Heart J 2010;31:1470–6.
22. Prati F, Regar E, Mintz GS, et al. Expert review document on methodology, terminology, and clinical applications of optical coherence tomography: physical principles, methodology of image acquisition, and clinical application for assessment of coronary arteries and atherosclerosis. Eur Heart J 2010;31:401–15.
23. Gonzalo N, Barlis P, Serruys PW, et al. Incomplete stent apposition and delayed tissue coverage are more frequent in drug-eluting stents implanted during primary percutaneous coronary intervention for ST-segment elevation myocardial infarction than in drug-eluting stents implanted for stable/unstable angina: insights from optical coherence tomography. J Am Coll Cardiol Intv 2009;2:445–52.

24. Jang IK, Tearney GJ, MacNeill B, et al. In vivo characterization of coronary atherosclerotic plaque by use of optical coherence tomography. Circulation 2005;111:1551–5.

25. Stamper D, Weissman NJ, Brezinski M. Plaque characterization with optical coherence tomography. J Am Coll Cardiol 2006;47:C69–79.

26. Di Mario C, Barlis P. Optical coherence tomography: a new tool to detect tissue coverage in drug-eluting stents. J Am Coll Cardiol Intv 2008;1:174–5.

27. Ozaki Y, Violaris AG, Kobayashi T, et al. Comparison of coronary luminal quantification obtained from intracoronary ultrasound and both geometric and videodensitometric quantitative angiography before and after balloon angioplasty and directional atherectomy. Circulation 1997;96:491–9.

28. de Feyter PJ, Ozaki Y, Baptista J, et al. Ischemia-related lesion characteristics in patients with stable or unstable angina. A study with intracoronary angioscopy and ultrasound. Circulation 1995;92:1408–13.

29. Kawasaki M, Takatsu H, Noda T, et al. In vivo quantitative tissue characterization of human coronary arterial plaques by use of integrated backscatter intravascular ultrasound and comparison with angioscopic findings. Circulation 2002;105:2487–92.

30. Sano K, Kawasaki M, Ishihara Y, et al. Assessment of vulnerable plaques causing acute coronary syndrome using integrated backscatter intravascular ultrasound. J Am Coll Cardiol 2006;47:734–41.

31. Yuan C, Zhang SX, Polissar NL, et al. Identification of fibrous cap rupture with magnetic resonance imaging is highly associated with recent transient ischemic attack or stroke. Circulation 2002;105:181–5.

32. Kolodgie FD, Gold HK, Burke AP, et al. Intraplaque hemorrhage and progression of coronary atheroma. N Engl J Med 2003;349:2316–25.

33. Tanaka A, Imanishi T, Kitabata H, et al. Morphology of exertion-triggered plaque rupture in patients with acute coronary syndrome: an optical coherence tomography study. Circulation 2008;118:2368–73.

34. Jang IK, Bouma BE, Kang DH, et al. Visualization of coronary atherosclerotic plaques in patients using optical coherence tomography: comparison with intravascular ultrasound. J Am Coll Cardiol 2002;39:604–9.

35. Takano M, Jang IK, Inami S, et al. In vivo comparison of optical coherence tomography and angioscopy for the evaluation of coronary plaque characteristics. Am J Cardiol 2008;101:471–6.

36. Inoue K, Motoyama S, Sarai M, et al. Serial coronary CT angiography-verified changes in plaque characteristics as an end point: evaluation of effect of statin intervention. J Am Coll Cardiol Img 2010;3:691–8.

37. Tahara N, Kai H, Ishibashi M, et al. Simvastatin attenuates plaque inflammation: evaluation by fluorodeoxyglucose positron emission tomography. J Am Coll Cardiol 2006;48:1825–31.

38. Tahara N, Kai H, Yamagishi S, et al. Vascular inflammation evaluated by [18F]-fluorodeoxyglucose positron emission tomography is associated with the metabolic syndrome. J Am Coll Cardiol 2007;49:1533–9.

39. Ohshima S, Fujimoto S, Petrov A, et al. Effect of an antimicrobial agent on atherosclerotic plaques: assessment of metalloproteinase activity by molecular imaging. J Am Coll Cardiol 2010;55:1240–9.

Key Words: atherosclerosis ▪ intravascular ultrasound ▪ ischemic heart disease ▪ optical coherence tomography ▪ plaque ▪ statin.